Disturbance recognition in the boreal forest using radar and Landsat 7

K.J. Ranson[1], K.Kovacs[2,] G. Sun[3], and V.I. Kharuk[4]

[1] NASA's Goddard Space Flight Center, Code 923, Greenbelt, MD, USA, jon@taiga.gsfc.nasa.gov
[2] Science Systems and Applications, Inc. Lanham, MD, USA, kkovacs@ltpmail.gsfc.nasa.gov
[3] Department of Geography University of Maryland, College Park, USA, guoqing@aspen.gsfc.nasa.gov
[4] V.N. Sukachev Institute of Forest, Academgorodok, Krasnoyarsk, Russia, kharuk@forest.akadem.ru

Abstract – As part of a NASA Siberian mapping project, this study evaluated the capability of three different radar sensors (ERS, JERS and Radarsat) and an optical sensor (Landsat 7) to detect fire scars, logging and insect damage in the boreal forest. Using images from each sensor individually and combined an assessment of the utility of using these sensors was developed. Transformed Divergence analysis revealed that Landsat data was the single best data type for this purpose. However, the combined use of the three radar and optical sensors did improve the results of discriminating these disturbances.

Introduction

Disturbance is an important factor in determining the carbon balance and succession of forests. Until the early 1990's researchers have focused on using optical or thermal sensors to detect and map forest disturbances from wild fires, logging or insect outbreaks. For example fires and scar can be detected using measured changes in temperature during the fire and the vegetation changes immediately after the burn (Kasischke et al. 1993, Martin 1993). Michalek et al. 2000 reported on the utility f TM data for assessing stand density and fire severity in Alaska.

Defoliation of forest stands results in changes in reflectance and can also be used to detect insect damage in forests. Insect damage studies have been reported in the literature using optical systems. Early work by Dottavio and Williams (1983) and Nelson (1983) demonstrated the utility of Landsat data for gypsy moth and spruce budworm damage in US forests. Landsat has also been studied to provide information on other insect outbreaks (Royle and Lathrop 1997, and Radeloff et al. 1999). A number of papers have appeared in the Russian literature describing

success of airborne and satellite systems to monitor insect outbreaks (e.g., Peretyagin et al. 1986, Kharuk, et al. 1989 and Karuk et al, 1998). There is a paucity of reported radar analysis of insect damage for boreal forests.

A problem with optical systems for northern forest studies was a lack of available data caused by cloud cover and low solar illumination in winter. The long term acquisition plan implemented with Landsat 7 and the lower cost of the data appears to have improved this situation.

With the launch of the synthetic aperture radar (SAR) systems: European Resource Satellite (ERS) -1 and 2, Japanese Earth Resources Satellite and Canada's Radarsat the problems of cloud cover and low illumination were eliminated. Kasischke et al. (1992) found ERS data could be used to detect fire scars in the boreal forest because the fire scars were 3-6 decibels (dB) brighter than the rest of the landscape. This brightness is a result of physical changes that occur due to fire including increased surface roughness, removal of tree canopies, and alteration of soil moisture patterns (Bourgeau-Chavez et al., 1993). While optical and thermal sensors are sensitive to the initial changes in temperature and vegetative cover, SAR is sensitive to the longer-term roughness and moisture patterns that occur post-fire. According to Kasischke et al. (1992) the burned area was not distinguishable from unburned forest using JERS data. They theorized that the lack of change on the L-band JERS images could be due to a lack of double bounce effect, or it could be due to the small size and geometry of the standing dead trees.

Much of the current work in disturbance mapping monitoring has employed the coarse resolution optical system Advanced Very High Resolution Radiometer (AVHRR). The frequent coverage is useful for detecting changes despite the 1.1 km resolution. SPOT vegetation and the NASA Earth Observing System MODIS instrument will also provide useful information. With the launch of Landsat 7 in 1999, implementation of a long term acquisition strategy and access to data from US and International Ground Stations, higher resolution optical data (30 m) has

become more readily available. The higher resolution data available from orbiting SARs also provides a closer look at disturbance patterns. While large area frequent coverage may not be practical, the detailed reflectance and backscatter can provide information useful for identifying type and extent of disturbances on a local to regional scale. This information can then be used with the coarser resolution systems to identify disturbance over large remote areas such as Siberia. This paper describes work towards understanding the use of remote sensing to detect important disturbance factors (fire scars and insect damage) in Siberia and explore the use of combined data from Landsat and SAR systems.

Study Sites

The general area of this forest disturbance study is located in central Siberia within 88-92 degrees East longitude and 50 to 70 degrees North latitude (Figure 1). Within this larger site are Landsat image sized (~180 X180 km) intensive study sites identified by their predominant disturbance. The Boguchany wild fire test site was selected because of the presence of large fire scars and logged areas in this location. The site is located at 97^{o} 25' E and 59^{o} 2' N, 75 km North of the Angara River and 350 km east of the Yenisey River in Eastern Siberia. The Priangar'e Insect site is located to the west of the Boguchany site 94˚ 30' E and 57˚ 30' N, and was plagued by a severe insect outbreak in the last decade.

The Boguchany test area, named after the nearby town, is located within an important region for timber logging in Siberia (Kharuk and Ranson 2000). The elevation of the study site ranges from 300 to 500 m. The growing season in the region is short, ranging from late May to Early September. In the summer, smoke plumes from burning wild fires obscure the sky; fire is the principal factor that determines ecosystem dynamics in this region and therefore most of the stands are of pyrogenic origin (Kharuk and Ranson, 2000). The Boguchany area is one of the main timber logging areas in the region. Pine (*Pinus* spp.) and Larch species (*Larix* spp.) cover most of this landscape, however other conifers, such as Siberian pine (*Pinus sibericus*), Spruces

(*Picea* spp.) and fir (*Abies* spp.), can also be found in patches in the area. Deciduous stands such as birch (*Betula* spp.) and aspen species (*Populus* spp.) cover the areas of lower elevation in this region. Several methods of logging are practiced in the area including the Finland technique (logging with seedlings preserved), and complete clearing where no vegetation is left on the site. These sites are covered with live grasses in the summer and covered with dry, dead grasses in the fall.

The fires that caused the burn scars in this study were ignited by lightening and extinguished by rainfall. This study will focus on the two largest fire scars in the area (See Fig. 2). Fire scar 1 is the product of two fires that were detected on the July 16 and 19, 1996 and merged into one fire the 21st of the same month. One of the two fires is known to have started on a 1979 clear-cut in an area of regenerating pine, birch and aspen when a large volume of dead wood ignited. The fire was a strong surface and crown fire and by the time it was extinguished on August 8, 1996, 32 thousand hectares of forest, old clear cuts and dense regenerating stands were burned. The second fire contributing to fire scar 1 started in an approximately 100 year old pine-larch stand that also included some regenerating pine and larch trees. Fire scar 2 burned in an undisturbed coniferous forest 60 km northwest from fire scar 1 also in 1996. The fire scars were located using satellite imagery and verified by field surveys in the fall of 1999 conducted by Scientist from the Sukachev Institute of Forest. Ground location was determined and survey plot measurements and digital on-ground photos were taken. IKONOS Carterra imagery was also available from the summer of 2001 for field checking.

The insect damage study site, as shown on Figure 3, is within the Niznee Priangar'e region where a severe Siberian silkmoth (*Dendrolimus sibiricus)* outbreak occurred. The topography of the area consists of a plateau with low hills. Soils are mainly spodosols (podzols). Climate is continental with cold dry winters and warm moist summers. Annual precipitation is 400-450 mm. Mean annual temperature is +2.6˚ C with an absolute minimum of -54˚ C recorded during

December and maximum of +36˚ C recorded in July. Vegetative growth period is about 100 days. Forests cover 95% of area. The dominant species are Siberian fir (*Abies sibirica*); other species included by Siberian pine (*Pinus sibirica*) also known locally as Siberian cedar, Siberian spruce (*Picea obovata*), Scotch pine (*Pinus silvestris*), larch (*Larix sibirica*), aspen (*Populus tremula*), and birch (*Betula verrucosa*). Stands are of average productivity with a wood stocking density of 200-230m^3/hectare and mean age of 135 years. Typical insect damage is characterized by complete defoliation and death of conifer stands, or death of only conifer trees within mixed stands.

Data and Preprocessing

Available JERS, ERS-1, Radarsat and Landsat-7 satellite data were analyzed to determine to what extent these sensors could detect the presence of fire scars, clear cuts and insect damage. Table 1 summarizes important parameters of the sensors used.

The JERS data were received from NASDA in the spring of 1999. The data were converted from slant to ground range and geocoded into the UTM projection by NASDA. At the Goddard Space Flight Center (GSFC) the data were resampled to 25 m pixel size, reoriented, and filtered using a 3 by 3 Frost filter (Frost *et al.* 1982, Lopes *et al.* 1990).

The ERS-1 data were received from the Alaska SAR Facility (ASF) in the spring of 1999. These data were then multilooked to 25 m pixel size at GSFC, reoriented, converted to ground range, wrapped onto a longitude/latitude grid using corner coordinates and, filtered using a 3 by 3 Frost filter.

The Radarsat standard beam data were received from ASF in January 2001 on 8mm tape in CEOS SAR file format. The data were previously converted to ground range by the ASF. At GSFC, the data were ingested, resampled to 25 m pixel size, wrapped into a longitude/latitude grid using corner coordinates and filtered using a 3 by 3 Frost filter. The Landsat 7 scenes were

ordered and received from the EOSDIS EROS Data Center Distributed Active Archive Center (DAAC) in the summer of 2000.

All image data were reprojected to the Lambert Conformal Conic (LCC) Projection with the WGS 84 datum. There was no radiometric terrain correction applied to the images because neither area had a steep topographic gradient (the elevation difference was less than 250 m). No additional atmospheric corrections were applied to the Landsat 7 data.

To attain greater geometric accuracy and to ensure that the data sets were co-registered with the highest possible accuracy, the JERS, ERS, and Radarsat data were registered to the Landsat 7 scene. Landsat 7 data were selected as geometric ground information for this site because these data have good geometric calibration. According to the Landsat 7 Project Science Office at the Goddard Space Flight Center, the absolute geodetic accuracy of Landsat 7 systematic product (generated without using ground control) is approximately 50 meters in the along and cross track directions, excluding terrain effects.

Ideally, orthorectification of radar images using a DEM should be performed before registration, but there was no high resolution DEM available. Instead we used a large number of control points to register the images. Because of the low terrain relief, the results seem satisfactory.

A manual registration step was also necessary because radar data from 3 different sensors could not be co-registered using corner coordinates alone with a high level of geometric precision. The SAR data was re-sampled and re-projected to the Lambert Conformal Conic Projection. Then, the SAR images were manually registered to the Landsat 7 scene. For this, points at the intersection of linear features were selected such as on roads, rivers, and clear cuts when applicable. In Boguchany, 103 points were used to register the ERS data, 74 to register JERS and 65 to register the Radarsat data. In Priangar'e 70 control points were used to register the JERS data and 90 to register the Radarsat data. The same procedure was used for both sites.

After registration, images were subsetted to the area covered by each of the 4 sensors. The smaller size and extent of the JERS image determined the final area for study. Figures 2 and 3 show the SAR and Landsat 7 images used for the analysis.

Methods

Vegetation classes

The following land cover classes were identified for the two sites: *coniferous forest (CF), broadleaf deciduous forest (DF), regeneration/sparse forest (RS), bare surfaces (BS) and clear cut (CC).* For the Boguchany site the following disturbance classes were added: *burned coniferous forest (BC), burned deciduous forest (BD), and burned logged areas (BL).* Additionally, two classes of insect damage were identified in the Priangare area: *severely damaged (SD)* with complete defoliation of a stand and *moderately damaged (MD*) with only conifer trees defoliated. Since the insect outbreak had occurred in 1996 and subsequently subsided the two classes represent severity of damage rather than stage of insect attack. Table 2 provides a list of classes and descriptions for the two study sites.

Training site selection

Field campaigns were conducted in the Boguchany area in the fall of 1999 and Priangar'e area in the summer of 2000. During this field campaigns, tree species were identified. GPS measurements were acquired and in Boguchany, plot measurements pertaining to the successional stages of the burned and logged areas were obtained. A field visit to Priangar'e included aerial overflights to obtain photography of damaged areas. Information gathered during these field campaigns along with the existing local ecological knowledge of the staff at the Sukachev Institute of Forest provided a good basis for determining and locating the different vegetation classes on the Landsat and radar images.

The training sites for the classes mentioned above were determined based on the information gathered in the field, the multi-year and multi-season coverage provided by other Landsat scenes

and the contextual information provided by the individual Landsat scenes. Once the training sites were so determined, histograms were examined for each class in each radar band. If the data was normally distributed, the class was left intact. If however the histogram showed a multimodal distribution, these training sites were displayed using the radar bands and training sites assigned to a more or less homogeneous subclass. Then the histograms for these subclasses were once again reviewed to make sure that the distribution of the values was normal. This way, the deciduous forest and bare ground classes was split into three subclasses on the Priangare site, and the burned-logged class were split into two subclasses on the Boguchany site. Approximately one-third of the training sites were set aside for testing the classification and two-thirds were used for training the classifier.

The clear cuts in both Boguchany and Priangar'e sites appear as rectangles with straight edges cut out of the forest cover in a checkerboard fashion revealing their man-made nature. The older clear cuts are clearly overgrown with deciduous trees, whereas the most recent ones have exposed bare soil. Because of the time difference between JERS and Landsat 7 data, only those logged sites were included in the clear cut class that were at least three years old and had grasses and seedlings growing on them. Based on *a priori* work, it was determined that the older, now tree covered clear cuts could not be separated from the natural deciduous forest cover. The fire scars in the Boguchany area are spatially quite distinct from the clear cuts. The fire scars have lobe-like edges that are at times discrete and at other times more transitional.

It is worth noting that if an unburned area is spectrally, structurally and texturally heterogeneous, it is likely that the fire scar visible in the landscape after burning will also be spectrally, structurally and texturally heterogeneous. This is to say that fire scars are not monolithic features at a 30m resolution. The patterns observable within a fire scar provide valuable information of the history of the site. When anthropogenic disturbance (such a logging) has occurred in the area prior to the burn, the burned area will be a patchwork of spectral,

structural and textural features shaped by a combination of anthropogenic and natural disturbance factors. This texture information was used to identify these sites but was not explicitly included in the classification.

On the Priangar'e site the logged areas do not appear in juxtaposition with the insect damage. In this case the anthropogenic (logging) and natural disturbances (insect infestation) are spatially separate. Insect damage appears on the landscape as patchy “thinned out” forested areas since insect only damaged the leaves of the coniferous trees and left the leaves of other trees intact. The degree of the damage they caused partly depends on the species composition of the stands: if a stand was composed of coniferous species, the stand was severely damaged. If the stand consisted of a mix of food and non-food species, then the damage was more moderate. It is important to mention that severely and moderately damaged classes are not thematically distinct. Instead they are two, somewhat arbitrarily defined overlapping areas on a thematic continuum between completely healthy and completely damaged forest stands.

Training sites for each class were chosen keeping in mind that the radar data available was acquired over a period of three years. The changes that have occurred within the landscape during this period had to be eliminated or at least minimized within the training sets. For example some of the Boguchany training sites were eliminated from the training set because on a 1991 Landsat 5 images they appeared as coniferous forest, and by the time the 1999 Landsat 7 scene was taken, the site became a clear cut. Since there was no additional information available on this particular site, it could not be determined at what point between the two dates the site was logged and whether or not the date of its logging fell within the three year period the radar data was acquired.

Data Analysis

The purpose of this analysis was to determine whether or not and how each sensor was detecting each land cover class and whether or not the radar sensors were capable of separating

the classes from one another based on backscatter information alone. Once the training sites were carefully selected and split into subclasses as described above, backscatter values were extracted from each class for each radar sensor, and descriptive statistics were generated. The analysis procedure consisted of two parts 1) Transformed Divergence (Richards and Jia, 1999) analysis and maximum likelihood classification. Transformed Divergence (TDM) is a measure of separability between classes and may therefore be used to assess the quality of the class spectral mean vectors and covariance matrices. A high TDM (> 1.80) indicates good statistical separation of the classes and indicates how well each sensor or sensor combination detected each land cover class. Maximum likelihood classification provides the means to examine the separability of classes in a mapping or thematic sense. After classification, the subclasses were merged into their original parent class.

Results and Discussion

Radar Data Analysis

Burned Site

Figure 4a presents the average backscatter and standard deviations for each radar sensor for the 7 classes from the Boguchany fire scar study area. For JERS data the coniferous and deciduous forest classes, as well as the burned deciduous and coniferous forest classes have very similar brightness values (see Figure 2a). This is probably because at L band (0.23 m wavelength), larger tree branches and trunks are the primary scatterers. After surface and crown fires, many of the tree trunks still remained standing as seen on the images of the burned forest sites. This might explain why the returns are so bright for both unburned and burned forest types in the L band. It is also clear that the regeneration sparse, clear cut and burned logged areas classes all have lower brightness values, which is likely due to the absence of large branches and trunks (see Figure 2). Classes with little or no tree cover (RS, CC and BL) also have similar backscatter and, as a group, have lower backscatter than the classes with standing trees.

In Figures 4a and 2 it can also be seen that the unburned classes (CF, DF, RS, and CC) all have lower ERS-1 brightness values than the burned classes (BC, BD, RS). The post-fire regeneration class seems to have intermediate values. C band radar is scattered by structures in about 5 cm in size such as leaves and small twigs on trees or grasses. Field observations revealed that small structures such as leaves and twigs were no longer present on burned trees, however grasses having leaves of that sizes are abundant on the fire scar during the summer months. Based on this, the burned and unburned vegetation should be difficult to distinguish, however, this is not the case. There must be some other factor such as soil moisture (Bourgeau-Chavez et al., 1993) influencing the CVV backscatter that causes the burned areas to be brighter than the unburned ones.

The plotted Radarsat backscatter shows very little difference between any of these classes (Figure 4a). Only the clear-cut class has backscatter values that are a bit lower than the others. These areas also appear dark on the radar image (Figure 2). There is not an obvious explanation as to why burned and unburned classes are so clearly separable using CVV ERS data and why the CHH Radarsat backscatter for these same classes are so similar. Only one year passed between the acquisition of the two data sets, therefore land cover change is unlikely be the answer. There is an 11^{o} difference in incidence angle between the two sensors, (ERS = 23^{o}, Radarsat = 34^{o}), but it is not well understood exactly how incidence angle influences radar backscatter from burned areas. Soil moisture could have changed over the one-year period and it is also possible that at a larger incidence angle, the differences in soil moisture between burned and unburned areas are less pronounced.

The separability of classes using the radar data was quantitatively examined with the use of the Transformed Divergence Measure (TDM). Table 3 lists the TDM values for all classes for the JERS, ERS and Radarsat data. For JERS data, high TDM values exist between logged classes (CC and BL) and unburned and burned conifer (CF, BC, respectively) and unburned and burned

deciduous stands (DF, BD, respectively). In this case, unburned forest stands are not separable from burned forest stands. High TDMs also exist between RS and BD classes. This indicates that forested classes and classes lacking tree cover are easily separable from each other using JERS data regardless of their burned state. ERS and Radarsat TDM values were generally lower than those for JERS. The exceptions were for ERS data which had much higher separability values for burned forest (BC and BD) and unburned forest (CF and DF).

From these results it is clear that any single radar sensor used alone cannot be used to discriminate between burned and unburned forest classes, between deciduous and coniferous forest classes, and between unburned and burned non-forested classes. However, JERS data can be used to discriminate between forest and non-forest classes regardless of burning, and between post-logging regeneration and forest classes also regardless of burning.

ERS data appears most useful for discriminating between burned forest areas and unburned forest, regeneration and clearings. Other class pairs with relatively high TDMs include RS and BC (1.49), and BD (1.73). This indicates that post-cutting regeneration is easily separable from the burned forest classes. However, the separability between the RS and the unburned forest classes (CF and DF) is very poor ($\leq$ 0.20). Low TDMs were found between CF and DF classes indicating that CVV data cannot be used to distinguish between coniferous and deciduous forest classes. TDM values were also minimal between CF and CC.

From these data it is clear that the CVV band alone cannot be used to discriminate between coniferous and deciduous stands, clear cuts and forest classes, and between clear cuts and post fire regeneration classes. However, ERS data can be used to discriminate between the burned and unburned land cover classes, regardless of other characteristics of the site, and between post cutting regeneration classes and burned forest classes. JERS data at the L-band seems to detect larger structural differences between forest types that are caused by logging (i.e. removal of large trunks). At the same time ERS C-band data seem to detect soil moisture differences (and perhaps

structural and moisture differences at a leaf level associated with burning). This indicates that the combination of the two sensors should provide improved results in discriminating logged and burned areas.

Table 3 shows the TDM values for the Radarsat data. The maximum separability is 0.72 and occurs between the CF and the CC classes. This value is quite low and indicates that the Radarsat data alone is not suitable for distinguishing any of these classes from each other.

Included in Table 3 are the TDM values generated based on the three sensor data combined. The average separability increased to 1.55. Although this is an increase from using each sensor alone (JERS average separability: 1.23, ERS: 0.64, and Radarsat: 0.16), on the whole, combining the three sensors does not provide very good distinction between these eight classes since TDM values under 1.8 are considered poor. Combining the radars provided the greatest increases in useful separability ($\geq$ 1.80) over individual radars between burned classes (BC, BD, BL) and regenerating forest (RS). Overall, forest (CF, DF) could be separated from disturbance classes (RS, CC, and BL), but not from burned forest (BC, BD). Burned forest could be separated from regeneration and clear cut. The common theme among class pairs is that classes can be separated successfully that have different structural characteristics determined by the presence or absence of large trunks and branches, such as forest and non-forest classes. This is mostly due to the LHH band JERS data, since these class pairs had reasonably high TDM values (around 1.7) using JERS data alone. ERS contributes the most in separating burned forest from other classes, however TDMs never reached 1.80 for any class pair.

Table 4 lists the maximum likelihood classification results of the combined radar data for the Boguchany site. Only the burned logged class (BL) was identified with accuracy greater than 80%. Forest classes were confused with each other as were burned forest classes. Regeneration and clear cut classes were mostly confused with each other. These classification results indicate that using this combination of radars might provide useful classification of forest classes (CF +

DF), logging (CC + RS), burned forest (BD + BD) and burned logged areas (BL). The overall classfication accuracy for all classes was about 66%.

Insect Damage Site

Figure 2b presents the average backscatter and standard deviations for the insect damaged site. Neither JERS nor Radarsat backscatter differs much across the forested sites (CF, DF, IS, IM). JERS backscatter decreases slightly for clear cuts and drops off for the bare surface class and water. Radarsat does not show this decrease in backscatter except for the water class. Apparently CC and BS surfaces are sufficiently rough to the C-band radar beam to maintain backscatter levels similar to forested sites.

Table 5 shows the radar separability values for the Priangar'e site. Two trends are obvious both JERS and Radarsat can distinguish water from the land cover classes very successfully, including the bare surface sub classes. JERS and, for the most part, Radarsat are also successful at distinguishing bare surfaces from the vegetated classes (1.92-2.00). Radarsat has low TDM values between bare surfaces and clear cuts and fails to separate the BA-2 class from all the vegetated classes. For JERS, TDM values are very low between coniferous forest (CF) and insect damage classes (IS, IM) and the deciduous forest subclasses and the moderate insect damage class. This might be because the insects only damage the leaves of the trees and the L band radar does not detect leaves, only major branches and trunks. Radarsat values are low for these classes, but higher than JERS for separating conifer forest from disturbance classes (IS, IM and CC).

Radarsat separability of the forests classes was poor ($\leq$ 1.31), as was separability of damaged forest classes from each other and with undamaged conifer forest ($\leq$ 0.97). The TDM values between deciduous subclasses and both damaged classes were also extremely low ($\leq$ 0.28). However the separability between coniferous forest and clear cuts was higher (1.77). This

may be because there is volume scattering occurring within the tree canopies while volume scattering back to the radar is absent from the grassy clear cuts.

With the combined use of the two radars the distinction between the clear cuts and coniferous forest (TDM=1.96) and clear cuts and severe insect damage (1.86) increased (Table 5). There was no large increase in the separabilities between the other classes. In addition, there was good separability of conifer forest and the deciduous subclass (DF3). Low TDMs were found for CF and the other two deciduous subclasses suggesting a possible mixture of conifer and deciduous trees or forest density differences among these deciduous classes. Overall, the combination of JERS and Radarsat maybe useful for separating clear cuts from other forest types, but is not useful for separating insect damaged stands from undisturbed forest.

The results of classification of the training sites using the JERS and Radarsat backscatter show 61% correct classification of conifer forest and 77% correct classification of the deciduous forest (combined subclasses). Reasonable classification results (> 80%) were obtained for clear cuts and bare areas and water (Table 6). Only 29% of the severely insect damaged, and 46% of the moderately damaged classes were classified correctly. Misclassifications were primarily with deciduous forest (51% and 41% respectively) indicating the combination of JERS and Radarsat is not useful for recognizing this disturbance.

Landsat and Combined SAR

Burned Site

Mean spectral reflectance digital numbers (DN) from burned area training sites are shown in Figure 5a. Only Bands 3 (0.63-0.69μm), 4 (0.76-0.90μm) and 5 (1.55-1.75 μm) are shown for illustration. Because of the post-senescence timing of the acquisition deciduous trees are bare and ground vegetation is dead reducing near-infrared (NIR) reflectance. Conifer forest has higher NIR response than burned conifer forest. Deciduous forest and burned deciduous forest exhibit a

similar trend but with higher responses. Clear cuts have unique spectral characteristics in this fall image with overall higher responses, especially in the SWIR (band 5).

The Landsat class separabilities for the burned site are shown in Table 7. The TDMs are greater than 1.80 for all classes except between burned forest classes (BC and BD) and between burned logged (BL-1 and BL-2) and clear cut (CC) classes. Regeneration (RS) and BL-1 TDM was slightly less than 1.80. Even though this Landsat 7 image was acquired in 1999, three years after the burn, many dead, burned trees still remained standing on the burned forested sites casting their shadows on the regenerating vegetation forest floor. This is why there is good distinction between the live and burned forest classes. One exception to this good separation between live and burned vegetation classes are the clear cut (CC) and the burned logged (BL) classes (TDM $\leq$ 1.45). The burned logged sites were logged prior to the burn in 1996. When the burn occurred, there were no trees standing on these sites, only grasses and seedlings. Since there was no mature trees on the site, there were no burned trunks left standing either that could cast their shadows on the regenerating grasses and seedling after the burn and therefore lower the site's reflectance in the NIR. This is why three years after the burn the burned logged site seems spectrally similar to a clear cut class and the regenerating/sparse class.

Using the Landast spectral statistics to classify the Boguchany burned area produced generally good accuracy. As shown in Table 8 conifer and deciduous forest classes, regeneration and the two burned forest classes had classification accuracies greater than 89%. Clear cut and burned logged areas were confused with each other resulting in lower classification accuracies of 83% and 84%, respectively. Overall accuracy was 90% and Kappa coefficient was 0.88 indicating Landsat reflective bands should perform well in discriminating the burned area classes.

As Table 7 shows, combining the three radars and Landsat data increased the TDM values for those classes that the optical and microwave sensors alone could not distinguish well. The

largest increase occurred in the case of the burned logged and burned deciduous class where TDM increased from 1.35 to 1.97 when the spectral and structural information was combined. However, there was only a minor increase in the TDM values between the clear cut and burned logged subclassess since in this case both classes were both spectrally (regenerating grasses and seedlings) and structurally (lack of trunks) similar.

In summary, L band radar data provided structural information of the vegetation such as the presence of absence of large trunks and C band radar data seems to provide information on soil moisture conditions while Landsat data provides spectral information on the vegetation cover such as whether or not the vegetation is reflective in the NIR. This synergistic interaction between the optical and microwave sensor is key to distinguishing disturbed sites from non-disturbed ones since they might look extremely similar using one or the other type of data alone.

Classification with fused data sets of Landsat, JERS, ERS and Radarsat resulted in classifcation accuracies above 90% for all classes (table not shown for brevity). The overall classification accuracy was nearly 94% with a Kappa coefficient of 0.93. The classes with the most improvement were the burned logged class (BL) from 84% to 93% and the CC class from 83% to 90%. The reduction of confusion between these two classes resulted in the higher classifcation accuracies. The added information on surface roughness condition available with the radar likely contributed here.

Insect Damage Site

Figure 5b shows that NIR reflectance are high for broad leaf trees and ground vegetation for the mid summer acquisition of the insect damaged area. The shorter wavelength reflectances (bands 1, 2 and 3, *vis* 3) did not vary much across the classes with vegetation in them. NIR and SWIR reflectances (Bands 4, 5 and 7, *vis* 4 and 5) however, are quite different and appear suited for discriminating forest classes from disturbed classes. Notice the overlapping spectral responses for the three deciduous subclasses. This is also apparent for the bare surface subclasses

except for TM band 4, suggesting a sparse vegetation cover on BA1 (more than on BA1 and BA2, but less than the clear cut (CC).

The widely varying spectral reflectances shown indicate that Landsat data can be used very successfully to distinguish among water, bare ground and clear cuts and all of the vegetation classes. Very high TDM values were observed between all class combinations indicating good separation of the forest classes and disturbances (Table 9). Even TDM values between severe and moderate insect damaged classes were high (1.83). The only low TDM values were found among subclasses of deciduous or among bare surface subclasses.

TDM results obtained after combining JERS, Radarsat and Landsat 7 for the insect disturbance area are also shown in Table 10. There was only modest improvement in TDM adding the radar data with the Landsat over the Landsat alone for most of the classes. However, combining the radar data with the Landsat data increased the separability between the severe and the moderately severe insect damaged classes from 1.83 to 1.93. Of interest is the increase in separability between DF-1 and DF-3 deciduous forest subclasses. Recall that the subclasses were selected from training sets originally selected from Landsat data, but yielded multimodal histograms with radar backscatter. DF-3 then is spectrally similar to DF-2 in the Landsat bands but apparently structurally dissimilar as inferred from the JERS backscatter. Based on this, DF-3 is likely a deciduous conifer or larch (*Larix* spp).

The classification results with Landsat 7 data were excellent as shown in Table 10. Every class had at least 95% classification accuracy. Overall accuracy was 98.6% with a Kappa coeffcient of 0.98. Adding the additional radar channels (results table not shown) offered only slight improvement in class accuracy with an overall 99% correct and kappa coefficient of 0.99.

Conclusions

This study was designed to examine the utility of using different radar systems and Landsat 7 for identifying forest landscape classes, especially those related to disturbance. We found that the

results were limited when using each single channel radar alone, however JERS and ERS were found to be useful for identifying certain classes. JERS was most useful for separating forest from disturbed classes with no standing trees. ERS was more useful for separating forest classes from disturbed classes where trees are left standing. Radarsat, on the other hand, was the least effective individual radar for this study. Combining the radars improved the identification of classes over results obtained with any single radar. Generally, if one radar sensor was found to have high separability for a pair of classes, adding additional radars did not greatly increase the separability. If all radars had low separability, combining the radars had very little benefit. In both sites the low separabilities found between CF and DF and burned forest and insect damaged forest classes indicates that classes that have both large trunks and leaves present on them are not possible to separate using even combined radar sensor data.

Regarding the detection of disturbance, the available data was acquired over a two-year period therefore careful comparison of radars for burn scar detection was not possible. Changes in surface soil moisture can greatly change the backscatter from burn scars as shown and verified by other researchers. We plan to continue to seek and analyze radar images acquired on similar dates to provide further information on this process.

Landsat 7 data proved the most useful of any single remote sensing system for recognizing forest type and discriminating between disturbance types. Even with non-growing season images, as was the case for the fire damaged site, the results were very promising. Combining the Landsat data with the available radar data improved the separability of classes and the overall classifications. The results also indicate that the combination of radar and Landsat 7 may be especially useful for recognizing other forest types by utilizing the structural information of radar and spectral information of Landsat 7. As radar and Landsat 7 data becomes more widely available combining these data sets should improve the accuracy of forest mapping activities. However, there is extra effort and cost involved in registering different image types.

This work underscores the importance of using multichannel SAR data for forest studies. The future ALOS and ENVISAT and Radarsat 2 multichannel systems may contribute greatly to improved results in forest analysis and disturbance mapping. When combined with optical data such as Landsat 7 there appears to offer potential for improving classifications.

Acknowledgment

This research was partially supported by NASA HQ Office of Earth Science NASA Grant NAG-5-3548 and RTOP 662-92.

References

Bourgeau-Chavez, L.L., Kasischke, E.S. and French N.H.F. (1993).Detection and interpretation of fire disturbed boreal forest ecosystems in Alaska using space born SAR data, *Proceeding of the Topical Symposium on Combined Optical-Microwave Earth and Atmosphere Sensing, Albuquerque, New Mexico*, New York: IEEE.

Dottavio, C.L., and Williams, D.L., (1983). Satellite technology- an improved means for monitoring forest insect defoliation. *Journal Forestry*, Vol.81, No.1, pp. 30-34.

Frost, V.S., Stiles, J.A., Shanmugan, K.S., and Holtzman, J.C. (1982). A model for radar images and its application to adaptive digital filtering of multiplicative noise, *IEEE Transactions on Pattern Analysis and Machine Intelligence*, Vol.4, No.2, pp.157-166.

Kasischke, E.S., French, N.H.F., Harrel, P.A., Christensen, N.L. Jr., Ustin, S.L., and Barry, D. (1993). Monitoring wild fires in boreal forests using large area AVHRR NDVI composite image data, *Remote Sensing of Environment*, Vol.45, pp.61-71.

Kasischke, E.S., Bourgeau-Chavez, L.L., French, N.H.F., Harrel, P.A., and Christensen, N.L. Jr. (1992). Initial observations on using SAR to monitor wild fire scars in the boreal forest, *International Journal of Remote Sensing*, Vol.13, pp.3495-3501.

Kharuk V.I., Peretyagin, G.I., and Palnikova, E.N. (1989). Automatic indication of pest outbreaks using false-color images, *Russian Journal of Remote Sensing*, Vol.5, pp.70-73 (in Russian).

Kharuk V.I., Isaev, A.S., and Kozukhovskaya, A.G. (1998). NOAA/AVHRR data in pest outbreak monitoring, *Russian Journal of Forestry*, Vol.4, pp.20-25 (In Russian).

Kharuk V.I., Ranson, K.J. (2000). Microwave fire scar detection. /In: *Biodiversity and dynamics of ecosystems in North Eurasia.* V.1. Part 2: *Biodiversity and Dynamics of Ecosystems in North Eurasia: Informational Technologies and Modeling.* (Novosibirsk, Russia, August 21-26, 2000). IC&G, Novosibirsk, pp.174-176.

Lopes, A., R. Touzi, and E. Nezry, (1990). Adaptive speckle filters and Scene heterogeneity, *IEEE Transactions on Geoscience and Remote Sensing*, Vol. 28, No. 6, pp. 992-1000.

Martin, P.M. (1993). Global fire mapping and fire danger estimation using AVHRR images, *Photogrammetric Engineering and Remote Sensing*, Vol.60, pp.563-570.

Michalek J.L., French N.H.F, Kasischke E.S., Johnson R.D., Colwell J.E. 2000Using Landsat TM data to estimate carbon release from burned biomass in an Alaskan spruce forest complex. *International Journal of Remote Sensing*, Vol. 21 No. 2, pp.323-338

Nelson, R.N. (1983). Detecting forest canopy change due to insect activity using Landsat MSS, *Photogrammetric Engineering and Remote Sensing*, Vol.49, pp.1303-1314.

Pereira, M.C., and Setzer, A.W. (1993). Spectral characteristics of fire scars in Landsat 5 TM images of Amazonia, *International Journal of Remote Sensing*, Vol.14, pp.2061-2783.

Peretyagin G.I., Kharuk, V.I., and Mashanov, A.I. (1986). Automatic classification of false-color images of larch stands damaged by pests, *Russian Journal of Remote Sensing*, Vol.2, pp.110-118 (in Russian).

Radeloff, V.C., Mladenoff, D.J. and Boyce, M.S. (1999). Detecting jack pine budworm defoliation using spectral mixture analysis: Separating effects from determinants, *Remote Sensing of Environ*ment, Vol.62, No.2, pp.156-169.

Richards J.A. and Jia, X. (1999). *Remote Sensing and Digital Image Analysis, An Introduction*, New York: Springer, pp.241-247.

Royle, D.D., and Lathrop, R.G. (1997). Monitoring hemlock forest health in New Jersey using Landsat TM data and change detection techniques, *Forest Science*, Vol.43, No.3, pp.ff-tt.

List of Figures.

Figure 1. Location of Boguchany burned site and Priangar'e insect damage site in Siberia

Figure 2.a. The JERS (LHH), b. ERS (CVV) c. Radarsat (CHH) and d. Landsat 7 images (Red = (NIR, 0.75 - 0.90 μm), Green = (Red, 0.63 - 0.69 μm), Blue= (Green, 0.525 - 0.605 μm) over the Boguchany site.

Figure 3.a. The JERS (LHH), b. Radarsat (CHH) and c. Landsat 7 images (Red = (NIR, 0.75 - 0.90 μm), Green = (Red, 0.63 - 0.69 μm), Blue= (Green, 0.525 - 0.605 μm) over the Priangar'e site. ERS data was not available for this site.

Figure 4. Mean and standard deviation backscatter coefficient for land cover classes at a) Boguchany burn scar and b.) Priangar'e Insect Damage site.

Figure 5. Means and standard deviations of Landsat 7 spectral digital numbers (DN) for land cover classes at a) Boguchany burn scar and b.) Priangar'e Insect Damage site.

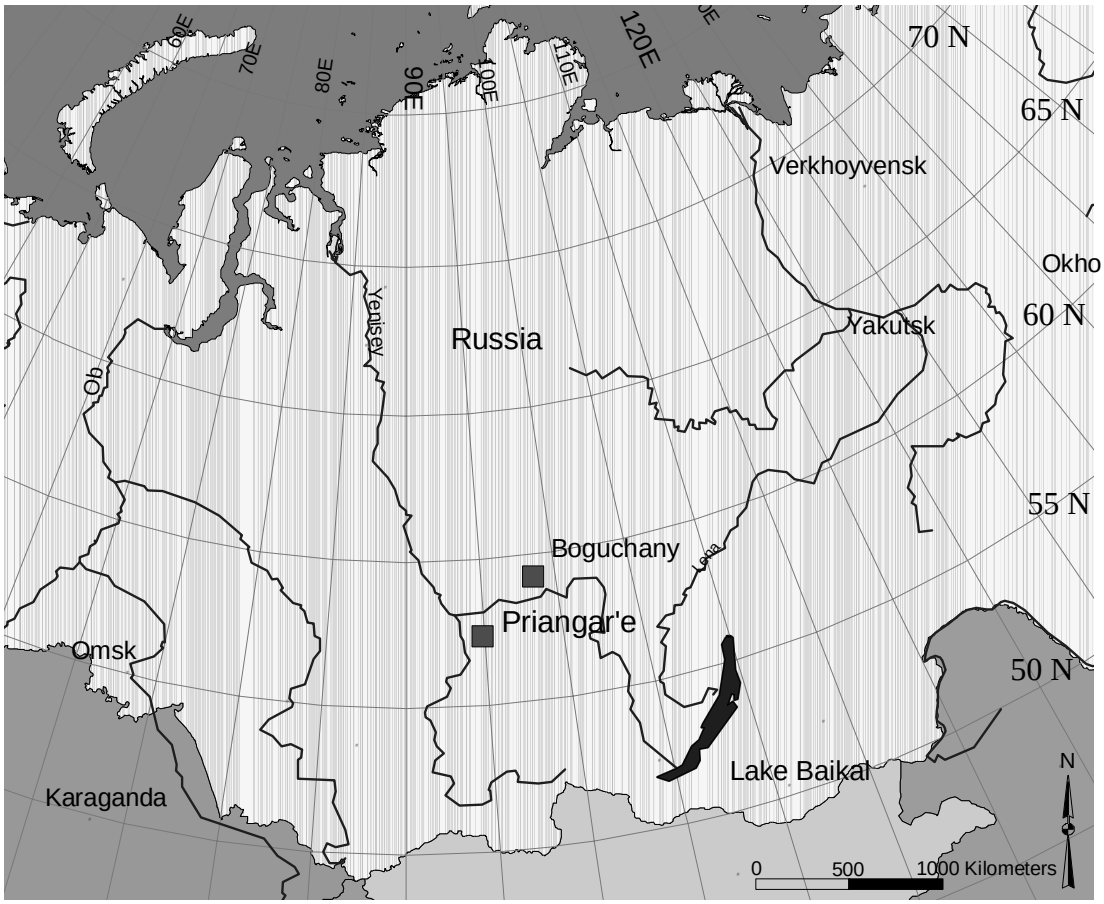

Figure 1: Location of Boguchany burned site and Priangar'e insect damage site in Siberia

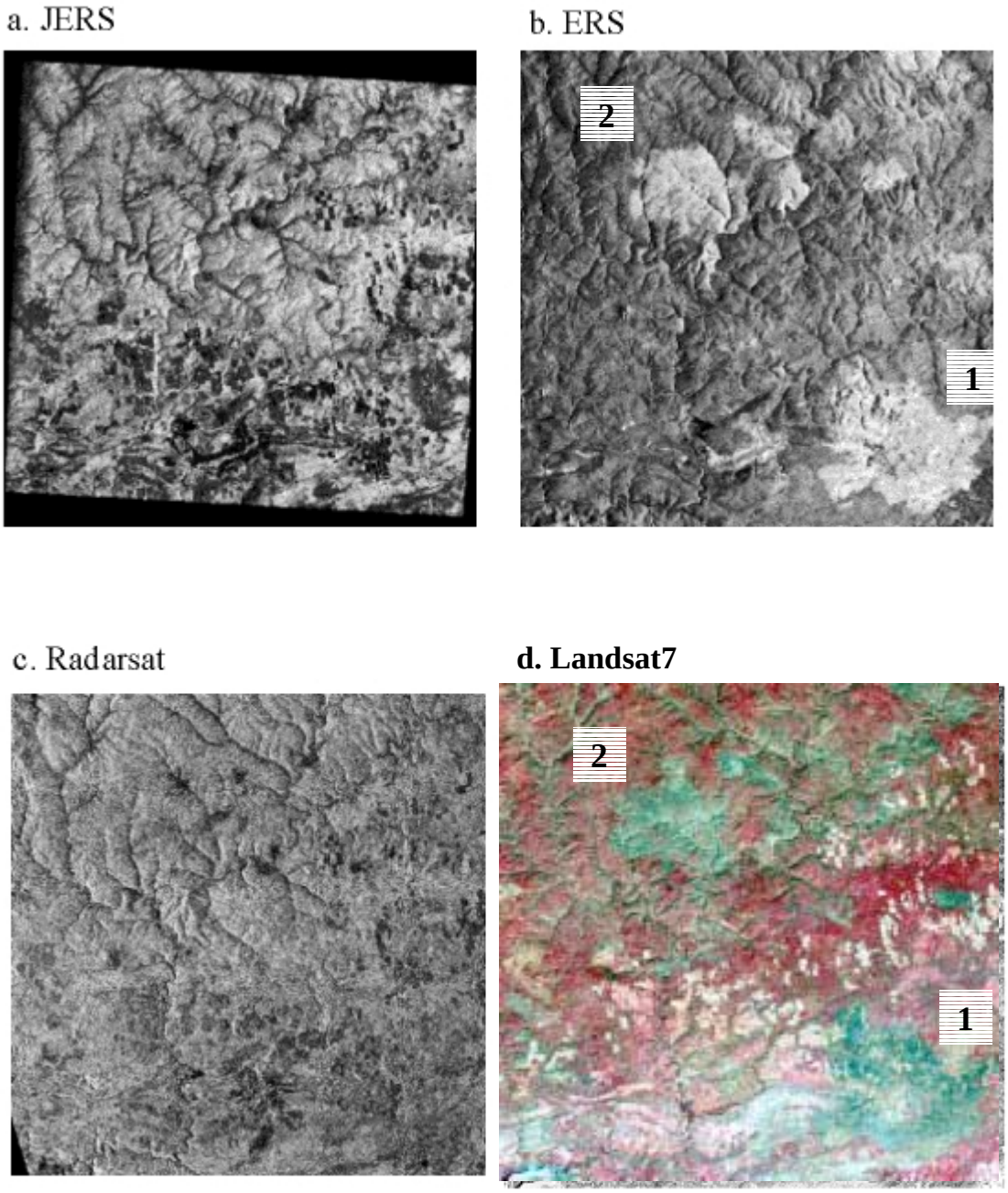

Figure 2.a: The JERS (LHH), b. ERS (CVV) c. Radarsat (CHH) and d. Landsat 7 images (Red = (NIR, 0.75 - 0.90 μm), Green = (Red, 0.63 - 0.69 μm), Blue= (Green, 0.525 - 0.605 μm) over the Boguchany site.

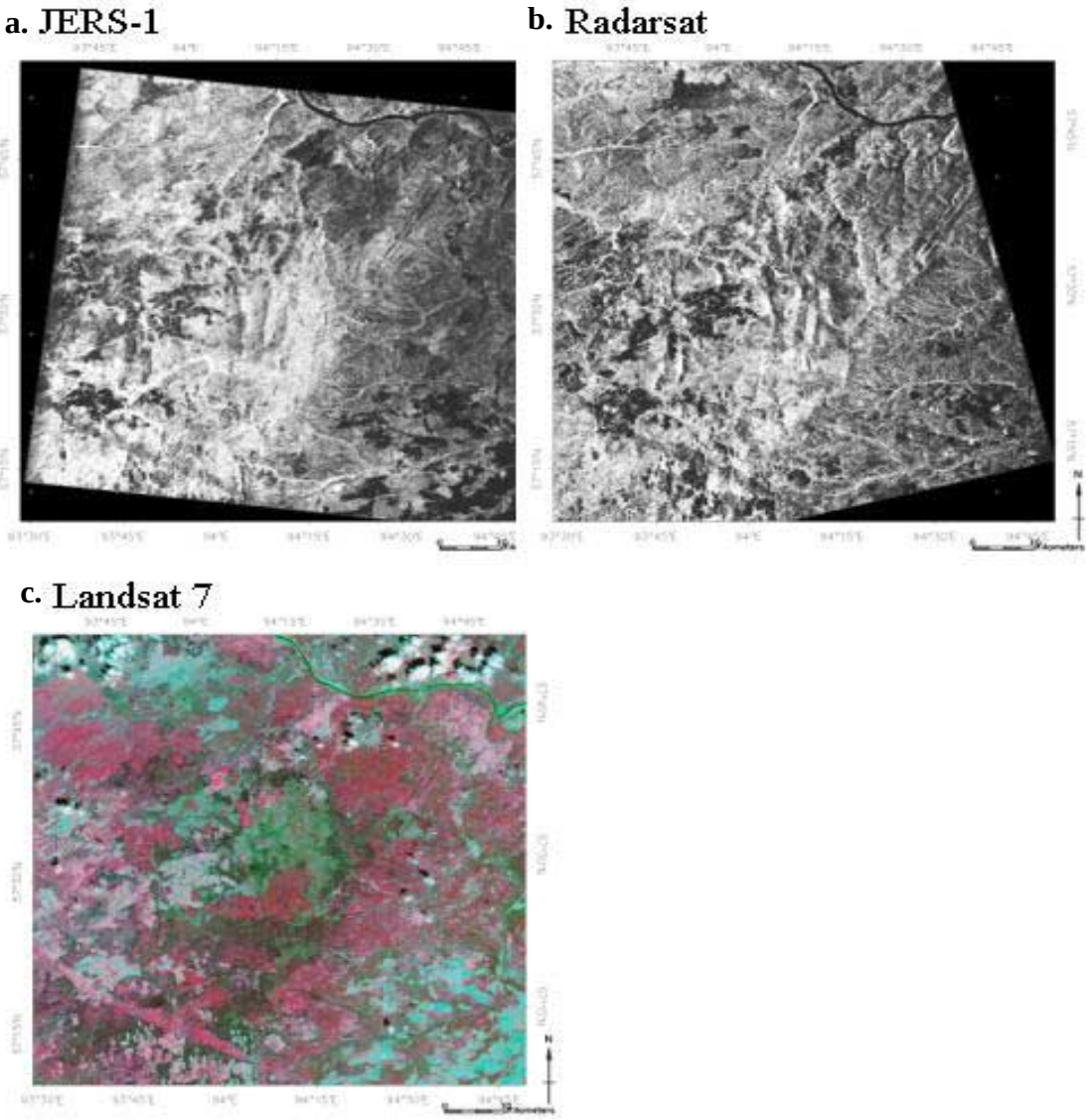

Figure 3.a: The JERS (LHH), b. Radarsat (CHH) and c. Landsat 7 images (Red = (NIR, 0.75 - 0.90 μm), Green = (Red, 0.63 - 0.69 μm), Blue= (Green, 0.525 - 0.605 μm) over the Priangar'e site. ERS data was not available for this site.

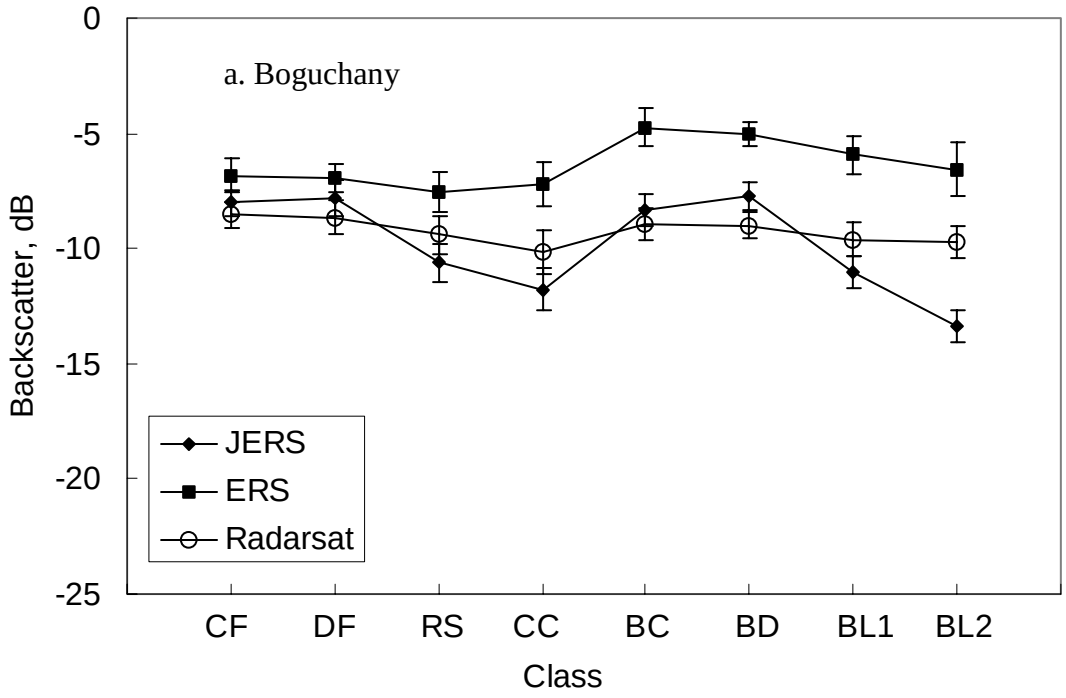

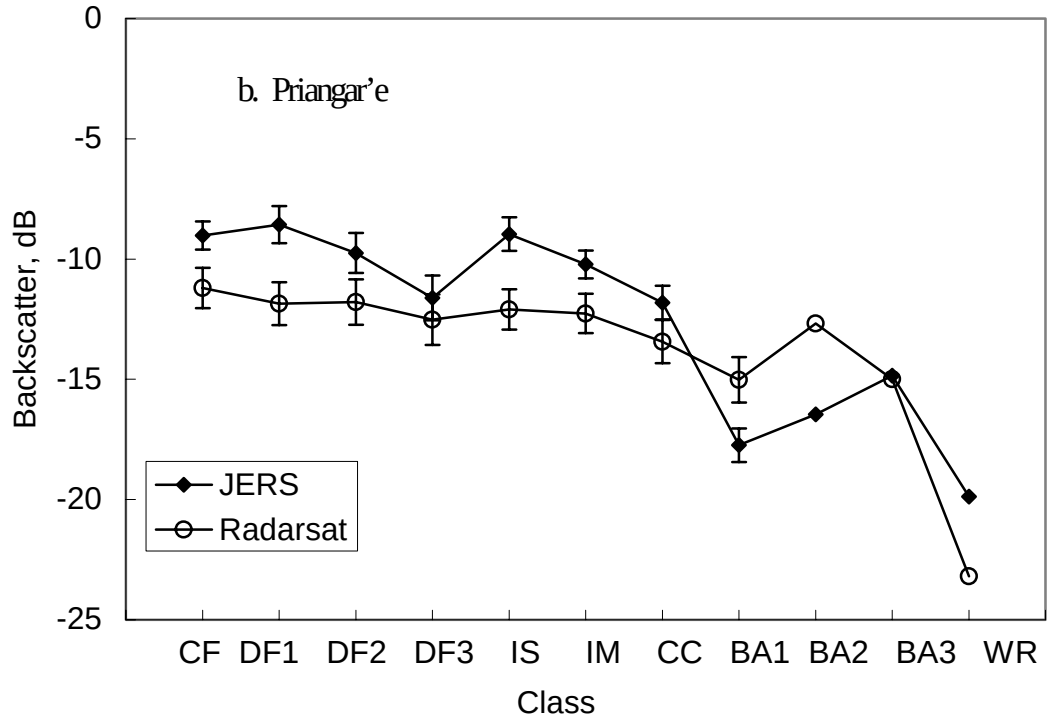

Figure 4: Mean and standard deviation backscatter coefficient for land cover classes at a.) Boguchany burn scar site and b.) Priangar'e Insect Damage site.

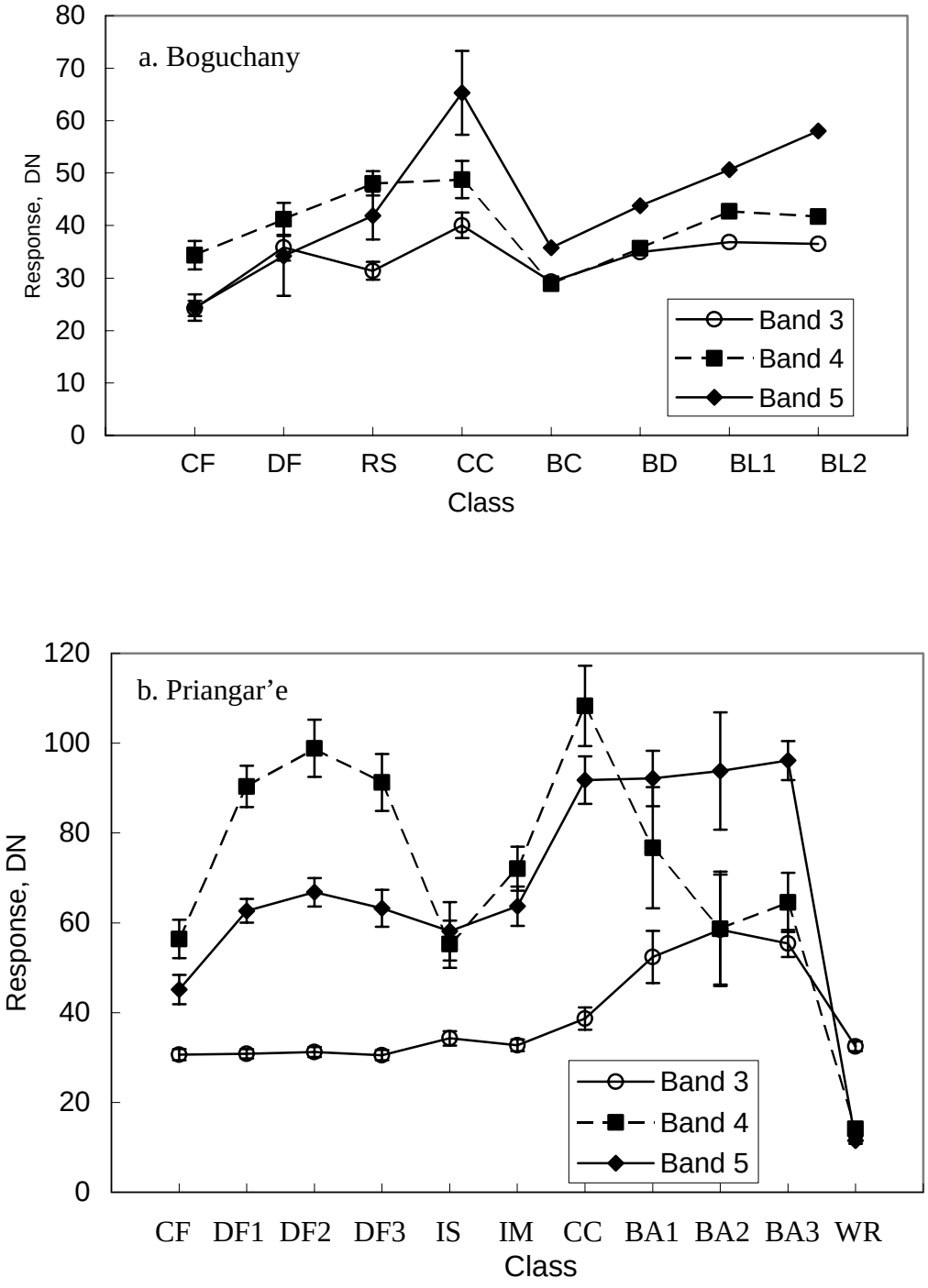

Figure 5: Means and standard deviations of Landsat 7 spectral digital numbers (DN) for land cover classes at a) Boguchany burn scar site and b.) Priangar'e Insect Damage site.

Table 1: Radarsat and Landsat data used for Boguchany and Priangar'e Sites.

Site	Boguchany			Priangar'e	
Sensor	JERS	ERS-1	Radarsat ST4	JERS	Radarsat ST4
Frequency (GHz)	L band (1.275)	C band (5.3)	C band (5.3)	L band (1.275)	C band (5.3)
Wavelength (cm)	23.5	5.66	5.66	23.5	5.66
Polarization	HH	VV	HH	HH	HH
Inc. angle (deg)	38.9^o	23^o	34^o	38.9	34
Image Center	58.01^{o}N, 97.43^{o}E	59.49^{o}N, 97.55^{o}N	59.10^{o}N, 97.33^o E	57.27^o N, 94.16^o E	58.01^o N, 93.86^o E
Orbital Direction	Descending	Descending	Ascending	Descending	Ascending
Image Swath (km)	75	100	100	75	100
Altitude (km)	580	785	798	580	798
Data take date	March 31, 1997	June 7,1998	Aug. 21, 1999	19-May-97	18-Aug-00
Pixel size (m)	12.5	12.5	12.5	12.5	12.5

Site	Boguchany	Priangar'e
Sensor	Landsat 7	
Data Take Date	Oct. 3, 1999	22-Jul-00
Image Center	58.71N, 96.81 E	57.31^o N, 94.36^o E
Path and Row	P141 R19	P140 R20
Resolution (m)	30	30
Sensor	ETM+	ETM+
Cloud cover (%)	0	9%
Bands	7 + pan	7 + pan

Table 2: Vegetation class and training set information. a) Boguchany Site, b) Priangar'e site a).

Class	Training pixel #	Testing pixel #	Class name	Description
CF	4184	1723	coniferous forest	Predominantly needle leaf species including larch
DF	4544	1361	deciduous forest	Predominantly broadleaf leaf species
RS	3593	1797	Regeneration/sparse	Site logged over 10 years ago, mixture of pine and deciduous seedlings
CC	3371	1210	Clear cuts	Recently logged stands with low vegetation cover of grasses and forbs.
BC	3679	1810	burned coniferous	Burned needle leaf species including larch
BD	3754	1675	burned deciduous	Burned broadleaf leaf species
BL	7459	1889	burned logged	Burned logged stands

b).

Class	Train pixel #	Test pixel #	Class name	Description
CF	7934	3836	Coniferous forest	Predominantly needle leaf species including larch
DF	7119	2663	Deciduous forest	Predominantly broadleaf leaf species
IS	6774	4082	Severe insect damage	Defoliated stands, few live trees
IM	3373	1809	Moderate insect damage	Stand with defoliated and undamaged trees.
CC	6191	3864	Clear cut	Recently logged stands with low vegetation cover of grasses and forbs.
BS	3384	1154	Bare surface	Non-vegetated areas may include roads, bare soil, fresh clear cuts, rock outcropping, bogs
WR	975	467	Water	Taseyeva River, tributary of the Angara river

Table 3: Transformed Divergence measure (TDM) values for vegetation classes and radar sensors (order of TDM values: JERS (J), ERS (E), Radarsat (R) and combining radar sensor data(C) for Boguchany.

class	Sensor	CF	DF	RS	CC	BC	BD	BL1
DF	J	0.06						
	E	0.01						
	R	0.01						
	C	0.10						
RS	J	1.69	1.58					
	E	0.20	0.24					
	R	0.20	0.15					
	C	1.74	1.64					
CC	J	1.94	1.88	0.38				
	E	0.08	0.14	0.04				
	R	0.56	0.48	0.12				
	C	1.97	1.92	0.57				
BC	J	0.06	0.11	1.39	1.82			
	E	1.18	1.40	1.49	1.23			
	R	0.04	0.02	0.06	0.36			
	C	1.35	1.54	1.86	1.95			
BD	J	0.05	0.04	1.80	1.97	0.20		
	E	1.35	1.48	1.73	1.55	0.18		
	R	0.06	0.04	0.05	0.33	0.01		
	C	1.40	1.53	1.96	1.99	0.37		
BL1	J	1.86	1.81	0.06	0.25	1.68	1.92	
	E	0.32	0.47	0.74	0.46	0.43	0.51	
	R	0.30	0.24	0.01	0.08	0.13	0.10	
	C	1.94	1.92	0.91	0.64	1.78	1.94	
BL2	J	1.99	1.99	1.63	0.86	1.99	1.99	1.54
	E	0.12	0.25	0.28	0.11	0.75	1.12	0.15
	R	0.38	0.31	0.03	0.03	0.19	0.16	0.01
	C	1.99	1.99	1.81	1.11	1.99	2.00	1.56
Average	J	1.23						
	E	0.64						
	R	0.16						
	C	1.55						

Table 4: Classification confusion table for Boguchany area classes and combined JERS. ERS, and Radarsat data. Average accuracy = 63.7, overall accuracy = 65.8%

	Percent Classified As						
Name	CF	DF	RS	CC	BC	BD	BL
CF	62.21	26.94	1.65	0.00	1.60	7.60	0.00
DF	46.96	45.69	2.29	0.00	0.11	4.78	0.18
RS	3.79	1.36	72.25	10.97	0.39	0.58	10.66
CC	0.09	0.18	19.25	52.65	0.00	0.00	27.82
BC	7.23	0.68	0.52	0.00	52.35	36.99	2.23
BD	3.76	2.53	0.03	0.00	17.05	76.27	0.37
BL	0.20	0.20	4.95	9.40	1.03	0.00	84.22

Table 5: TDM values for Priangar'e insect damage study site for. JERS (J) and Radarsat (R) and combined data (C).

Class	Sensor	CF	DF1	DF2	DF3	IS	IM	CC	BA1	BA2	BA3
DF1	J	0.47									
	R	0.59									
	C	0.92									
DF2	J	0.49	1.18								
	R	0.45	0.01								
	C	1.04	1.22								
DF3	J	1.77	1.98	1.52							
	R	1.31	0.57	0.61							
	C	1.88	1.99	1.75							
IS	J	0.06	0.26	0.45	1.84						
	R	0.65	0.15	0.15	0.18						
	C	0.72	0.45	0.59	1.86						
IM	J	0.53	1.49	0.19	0.93	0.69					
	R	0.97	0.25	0.28	0.07	0.04					
	C	1.32	1.62	0.59	1.04	0.74					
CC	J	1.50	1.97	1.43	0.07	1.70	0.76				
	R	1.78	1.46	1.46	0.59	0.91	0.85				
	C	1.96	1.99	1.95	0.78	1.86	1.42				
BA1	J	2.00	2.00	2.00	1.99	2.00	2.00	1.99			
	R	1.99	1.98	1.99	1.92	1.92	1.95	1.20			
	C	2.00	2.00	2.00	2.00	2.00	2.00	1.99			
BA2	J	2.00	2.00	2.00	1.99	2.00	1.99	1.96	0.54		
	R	1.42	0.76	0.79	0.02	0.28	0.17	0.40	1.85		
	C	2.00	2.00	2.00	1.99	2.00	2.00	1.97	1.95		
BA3	J	2.00	2.00	2.00	1.99	2.00	2.00	1.99	1.92	1.29	
	R	2.00	2.00	1.99	1.98	1.97	1.95	1.51	0.25	1.95	
	C	2.00	2.00	2.00	2.00	2.00	2.00	2.00	1.93	1.99	
WR	J	2.00	2.00	2.00	2.00	2.00	2.00	2.00	1.87	1.99	2.00
	R	2.00	2.00	2.00	2.00	2.00	2.00	1.99	1.98	1.99	1.99
	C	2.00	2.00	2.00	2.00	2.00	2.00	2.00	2.00	2.00	2.00
Avg.	J	1.58									
	R	1.23									
	C	1.73									

Table 6: Classification confusion table for Priangar'e area classes and JERS and Radarsat combined data. Average Accuracy = 62.48%, Overall accuracy = 70.71

	Percent Classified As							
Name	NULL	CF	DF	IS	IM	CC	BA	WR
CF	0.00	61.44	36.50	0.52	1.54	0.00	0.00	0.00
DF	0.00	4.77	77.42	4.09	8.51	5.21	0.00	0.00
IS	0.00	9.71	51.34	29.57	9.24	0.13	0.00	0.00
IM	0.00	0.80	40.76	10.91	46.13	1.39	0.00	0.00
CC	0.00	0.08	14.00	0.19	4.28	81.39	0.05	0.00
BA	0.09	0.00	0.00	0.00	0.00	0.89	99.03	0.00
WR	0.00	0.00	0.00	0.00	0.00	0.00	0.00	100.00

Table 7: TDM separabilities for Landsat 7 (L) and combined Landsat and SAR (C) data for Boguchany classes

Class	Sensor	CF	DF	RS	CC	BC	BD	BL1
DF	L	1.99						
	C	1.99						
RS	L	1.99	1.91					
	C	1.99	1.98					
CC	L	2.00	1.99	1.82				
	C	2.00	2.00	1.89				
BC	L	1.99	1.99	2.00	1.99			
	C	2.00	1.99	2.00	2.00			
BD	L	2.00	1.99	1.98	1.98	1.77		
	C	2.00	1.99	1.99	2.00	1.84		
BL1	L	2.00	1.94	1.79	1.45	1.96	1.35	
	C	2.00	1.99	1.89	1.65	1.99	1.97	
BL2	L	2.00	1.99	1.99	1.29	1.95	1.75	1.01
	C	2.00	2.00	1.99	1.68	2.00	2.00	1.76
Avg.	L	1.85						
	C	1.95						

Table 8: Classification confusion table for Boguchany area classes and Landsat 7 data. Average accuracy = 91.10, overall accuracy = 90.55%

Percent Classified As

Name	CF	DF	RS	CC	BC	BD	BL
CF	98.35%	1.60%	0.05%	0.00%	0.00%	0.00%	0.00%
DF	1.01%	94.89%	2.68%	0.00%	0.04%	0.07%	1.30%
RS	0.22%	2.59%	92.32%	3.73%	0.00%	0.00%	1.14%
CC	0.00%	0.12%	2.17%	83.06%	0.00%	0.00%	14.65%
BC	0.03%	0.49%	0.16%	0.00%	95.90%	2.58%	0.85%
BD	0.00%	0.32%	0.43%	0.00%	3.30%	89.00%	6.95%
BL	0.00%	0.44%	0.87%	8.48%	1.56%	4.45%	84.21%

Table 9: TDM separabilities from Landsat 7 and combined Landsat and SAR (C) data for Priangar'e classes

Class	Sensor	CF	DF1	DF2	DF3	IS	IM	CC	BA1	BA2	BA3
DF1	L	1.99									
	C	1.99									
DF2	L	1.99	1.06								
	C	2.00	1.73								
DF3	L	1.99	0.26	1.09							
	C	2.00	1.99	1.88							
IS	L	1.98	2.00	2.00	2.00						
	C	1.98	2.00	2.00	2.00						
IM	L	1.97	1.96	1.98	1.96	1.83					
	C	1.98	1.99	1.99	1.98	1.93					
CC	L	2.00	2.00	2.00	2.00	2.00	2.00				
	C	2.00	2.00	2.00	2.00	2.00	2.00				
BA1	L	2.00	2.00	2.00	2.00	2.00	2.00	1.99			
	C	2.00	2.00	2.00	2.00	2.00	2.00	2.00			
BA2	L	2.00	2.00	2.00	2.00	2.00	2.00	2.00	1.76		
	C	2.00	2.00	2.00	2.00	2.00	2.00	2.00	2.00		
BA3	L	2.00	2.00	2.00	2.00	2.00	2.00	2.00	1.64	1.93	
	C	2.00	2.00	2.00	2.00	2.00	2.00	2.00	1.99	2.00	
WR	L	2.00	2.00	2.00	2.00	2.00	2.00	2.00	2.00	2.00	2.00
	C	2.00	2.00	2.00	2.00	2.00	2.00	2.00	2.00	2.00	2.00
Avg.	L	1.73									
	C	1.99									

Table 10: Classification confusion table for Priangar'e area classes Landsat 7data. Average Accuracy = 98.18%, Overall accuracy = 98.14%

	Percent Classified As						
Name	CF	DF	IS	IM	CC	BA	WR
CF	99.04%	0.03%	0.53%	0.40%	0.00%	0.00%	0.00%
DF	0.01%	99.61%	0.00%	0.32%	0.06%	0.00%	0.00%
IS	0.52%	0.00%	96.22%	2.23%	0.01%	1.02%	0.00%
IM	0.06%	1.46%	1.87%	95.61%	0.03%	0.98%	0.00%
CC	0.00%	0.02%	0.00%	0.00%	98.34%	1.65%	0.00%
BA	0.00%	0.00%	0.03%	0.00%	1.45%	98.43%	0.00%
WR	0.00%	0.00%	0.00%	0.00%	0.00%	0.00%	100.00%

List of Tables